Herpetologica, 79(4), 2023, 196–206

They Might Be Giants: Divergence in Display Structure Between Two Island Populations of Galápagos Lava Lizards (*Microlophus bivittatus*)

Joseph M. Macedonia[1,6,7], David L. Clark[2,6], Morgan R. Fonley[3], John W. Rowe[2], Emma E. Neyer[2], Emilio J. Mancero[4], and Carlos A. Valle[5]

[1] Department of Biology, Florida Southern College, Lakeland, FL 33801, USA
[2] Department of Biology, Alma College, Alma, MI 48801, USA
[3] Department of Mathematics, Alma College, Alma, MI 48801, USA
[4] Biology Department, Grand Valley State University, Allendale, MI 49401, USA
[5] Colegio de Ciencias Biológicas y Ambientales COCIBA & Galápagos Science Center GSC, Universidad San Francisco de Quito, Ecuador

Abstract: The geographic isolation of conspecific populations can produce a diversification of signals through genetic drift, which may be reinforced by selection if populations (or sibling species) come into secondary contact. As conspicuous visual signals, bobbing displays of lizards have been described for numerous genera, and differences in display structure have been documented between some isolated conspecific populations. Although bobbing display structure has been detailed for several Galápagos Lava Lizard species (*Microlophus* sp.), intraspecific populations on different islands also exhibit various degrees of display structure divergence. In the present study, our goal was to determine if *Microlophus bivittatus* on San Cristóbal Island and a population on its adjacent islet of Isla Lobos possess differences in bobbing display structure. Interestingly, adult males on Isla Lobos exhibit gigantism compared to those on San Cristóbal, and the two populations have been isolated by the sea for several thousand years. We predicted that bobbing display speed would scale inversely with body size, such that displays would be detectably slower and longer in the supersized Isla Lobos males than those in the smaller San Cristóbal males. To test this prediction, we elicited displays from subjects by using a conspecific-mimicking robot. We measured two displays from 16 subjects in each population by using conventional unit-based variables as well as Fourier transform-based variables. After determining correlations among display variables, we tested for differences in uncorrelated display unit durations between Isla Lobos and San Cristóbal males. We then quantified within-subject, among-subject, and between-population variance for all variables by using nested ANOVAs and tested if variance differed between study populations at any level. Next, we used principal component analysis to create a small number of normally distributed variables (i.e., the principal components) from our original variables. These principal components then were used as inputs for discriminant function analysis to classify displays to populations. Comparisons of display unit durations supported our prediction only for the initial bob in displays, which was longer in Isla Lobos males than in San Cristóbal males. Nevertheless, when we considered multiple variables collectively, discriminant function analyses classified displays to the correct population at a level significantly greater than chance in all four unit-based analyses and three of four discrete Fourier transform-based analyses. Finally, supported by data on sexual size dimorphism and genetic differences between pairs of *M. bivittatus* populations (F_{ST}), our results indicate that divergence in bobbing display structure can occur relatively quickly if populations are sufficiently isolated.

Key words: Discriminant function analysis (DFA); Discrete Fourier transform (DFT); Lizard displays; Principal components analysis (PCA); Population divergence; Sexual dimorphism index (SDI); Sexual size dimorphism (SSD)

The ritualized visual displays of animals that occur in the contexts of courtship and male–male competition are astonishingly varied (Darwin 1871; Bradbury and Vehrencamp 2011; Eliason 2018). In some highly diverse taxa, such as birds of paradise (Irestedt et al. 2009; Ligon et al. 2018), *Anolis* lizards (Losos et al. 1998; Losos 2009; Mahler et al. 2010, 2013), and peacock spiders (Girard et al. 2021), species-specific displays of color and motion are prime examples of sexual selection and, frequently, of allopatric speciation (Tinghitella et al. 2018). The geographic isolation of conspecific populations also can produce visual signal differentiation through genetic drift (e.g., Kronforst and Gilbert 2008). Examples of population divergence in visual signals are numerous, but a few notable cases in amphibians include color pattern variation in the strawberry poison frog (*Oophaga pumilio*; Siddiqui et al. 2004; Rudh et al. 2011; Cummings and Crothers 2013; Gehara et al. 2013; Richards-Zawacki and Cummings 2014; Guillory et al. 2019) and in the dyeing poison frog (*Dendrobates tinctorius*; Noonan and Gaucher 2006). Among invertebrates, color and motion signal variations are particularly striking in the Arizona sky island jumping spider (*Habronattus pugillis*; Masta and Maddison 2002; Eilas et al. 2006). In addition, visual signal divergence may be reinforced if formerly isolated populations or sibling species come into secondary contact, as has been argued for (1) the facial color patterns of guenons (Allen et al. 2014), (2) dewlap color and electrophoretic variation in the *Anolis brevirostris* complex (Webster and Burns 1973; Lambert et al. 2013) and, at least in part, (3) dewlap color and genomic variation in *Anolis distichus* (Ng and Glor 2011; Ng et al. 2017).

As conspicuous visual signals, species-specific bobbing displays have been described for numerous lizard genera, and the divergence of display structure has been documented among conspecific populations within many of those genera (Supplemental Table S1, available online). Display structure can change via modifications in the elevation and speed of head vertical displacement, as well as in the complexity of the head motion sequence (Carpenter 1966; Jenssen 1977). Conventionally, lizard bobbing displays are visualized by plotting them as display action pattern graphs (Carpenter and Grubitz 1961). Once graphed, a display is parceled into units, where attributes such as unit durations, bob amplitudes, and other features may be measured (Clark et al. 2015). An alternative approach that we have used previously to quantify lizard

[6] Authors contributed equally to this study.
[7] Correspondence: e-mail, Joe.Macedonia@gmail.com

bobbing displays is Fourier transform (Fleishman 1986, 1988; Macedonia et al. 2019, 2021). This method allows us to analyze displays as a whole (cf., units), by deconstructing them into a series of sinusoidal waves.

Bobbing display structure is highly distinctive among Galápagos Lava Lizard species (Carpenter 1966; Clark et al. 2015, 2016; Macedonia et al. 2019). More subtle structural differences also occur, however, between some pairs of geographically separated conspecific populations (Carpenter 1966; Clark et al. 2015). For example, although no differences in display structure have yet been reported for *Microlophus albemarlensis* on Isabella and Fernandina Islands (population divergence < 30 kyr; Benavides et al. 2009), slight structural differences occur between *Microlophus jacobi* on the islands of Santiago and Rábida (estimated time since divergence unknown or unpublished) and are moderate between *Microlophus indefatigabilis* on the islands of Santa Cruz and Santa Fé (population divergence approximately 400 kyr; Benavides et al. 2009; Clark et al. 2015).

In this study we compare bobbing display structure in *M. bivittatus* on the island of San Cristóbal and on its adjacent islet, Isla Lobos. The time of divergence for these two populations has not been established, but extrapolation from Ali and Aitchison (2014: their Fig. 2) and estimates of sea level rise during the past 5 kyr (Poulos et al. 2009) suggest that the two locations are separated by just a few thousand years. Despite being divided by a water channel only about 300-m wide on average, adult male *M. bivittatus* individuals are strikingly larger on Isla Lobos than those on San Cristóbal (Supplemental Fig. S1, available online). Thus, in addition to display structure, we compare body size and sexual size dimorphism (SSD) of our study species on the two islands. The island-specific differences in male body size led us to consider that bobbing display speed might, at least to some degree, scale inversely with size (see Dial et al. 2008 for a review). We, therefore, predicted that the supersized Isla Lobos males would exhibit longer display unit durations and greater total display durations than the smaller-bodied San Cristóbal males.

Materials and Methods

Subjects and Study Area

Microlophus bivittatus is restricted to the Galápagos Island of San Cristóbal and its nearby islet, Isla Lobos. The direct distance between adjacent coastlines of the two islands ranges roughly from 165 to 345 m (Google Maps 2023; Google, Mountain View, CA). On San Cristóbal, *M. bivittatus* inhabits flat coastal beach areas as well as upland habitats. These habitats exhibit variable degrees of vegetation cover and vertical spatial stratification, as determined by extensive lava rock formations, shrubs, and forest. Our study of bobbing display behavior on San Cristóbal was conducted in and around Puerto Baquerizo Moreno (longitude: –89.61434, latitude: –0.90920; datum WGS84 in all cases). For the body size and SSD comparisons, we captured males and females by noose or by hand on San Cristóbal in a beach habitat at Playa Ochoa (longitude: –89.57083, latitude: –0.86333) and an upland habitat at Punta Carola (longitude: –89.61027, latitude: –0.89111). On Isla Lobos (longitude: –89.56583, latitude: –0.85583), our study species primarily occupied a sandy beach habitat with scattered small rocks, dense low-shrub vegetation, and few trees. In southwestern San Cristóbal, Playa Ochoa is approximately 1.0 km southwest of Isla Lobos, whereas Punta Carola is about 6.4 km southwest of Isla Lobos (Google Maps 2023; Google).

For each lizard, we obtained snout–vent length (SVL) to the nearest 1 mm by using a plastic ruler and calculated SSD indices for lizards at each location (Gibbons and Lovich 1990; Lovich and Gibbons 1992). We measured 121 females and 104 males across the 3 study sites, totaling 225 individuals. Each lizard received a unique passive integrated transponder tag (HPT9; Biomark) and was released unharmed at the site of capture within hours. Using JMP (SAS Institute, Cary, NC), we natural log transformed SVL data and analyzed them with a 2×3 factorial ANOVA, with sex and study location as main effects, and their interaction. Post-hoc comparisons were conducted using multiple contrasts of adjusted means.

Bobbing Display Data Collection

Microlophus bivittatus produces the following two types of bobbing displays: brief two-bob displays, which occur immediately before locomotion (Clark et al. 2017, 2019, 2023; Macedonia et al. 2019), and species-specific signature displays (Stamps and Barlow 1973; Jenssen 1977, 1978), which are produced by most Iguania taxa during same-sex competition, courtship, and male nondirected broadcast of territorial ownership. The present study is restricted to an analysis and comparison of signature displays from male *M. bivittatus* on San Cristóbal and on Isla Lobos.

Bobbing displays were recorded with a video camera (Panasonic HC-WX970 WiFi camcorder) mounted on a tripod, as well as a cell phone camera (Samsung S21 + 5G) with a high-resolution video format (H.264). For the hand-held phone camera, any motion that was not due to lizard vertical body displacement during bobbing was corrected manually frame-by-frame to a reference pixel by using the image stabilization filter in Apple iMovie (v10.2.3; Apple Inc., Cupertino, CA). This process provided a video image as stable as that obtained with a tripod-mounted video camera.

We cataloged the occurrence of bobbing displays while reviewing robot trial footage and extracted and saved display clips as MP4 files in QuickTime Player (v10.5; Apple Inc.). Next, the video clips were imported into an open-source video analysis program, Tracker (v6.0.1; Brown et al. 2021). We used the object-tracking function and gathered frame-by-frame vertical coordinates of head motion by placing the cursor over a subject's eye and clicking a computer mouse. The vertical coordinates then were exported to Microsoft Excel (v26.57, Microsoft Corporation, Redmond, WA) where time (x-axis) and amplitude (y-axis) measurements of the displays could be made.

We selected two signature displays of high video quality (i.e., close focus of a nonobscured subject in response to a robotic conspecific) for 16 males of each study population to compare display structure. Although male and female lava lizards from the same population produce structurally identical signature displays (Carpenter 1966; Clark et al. 2017, 2023), we chose males as subjects because the large difference in male body size on the two islands allowed us to test our prediction that display speed and body size would be inversely related.

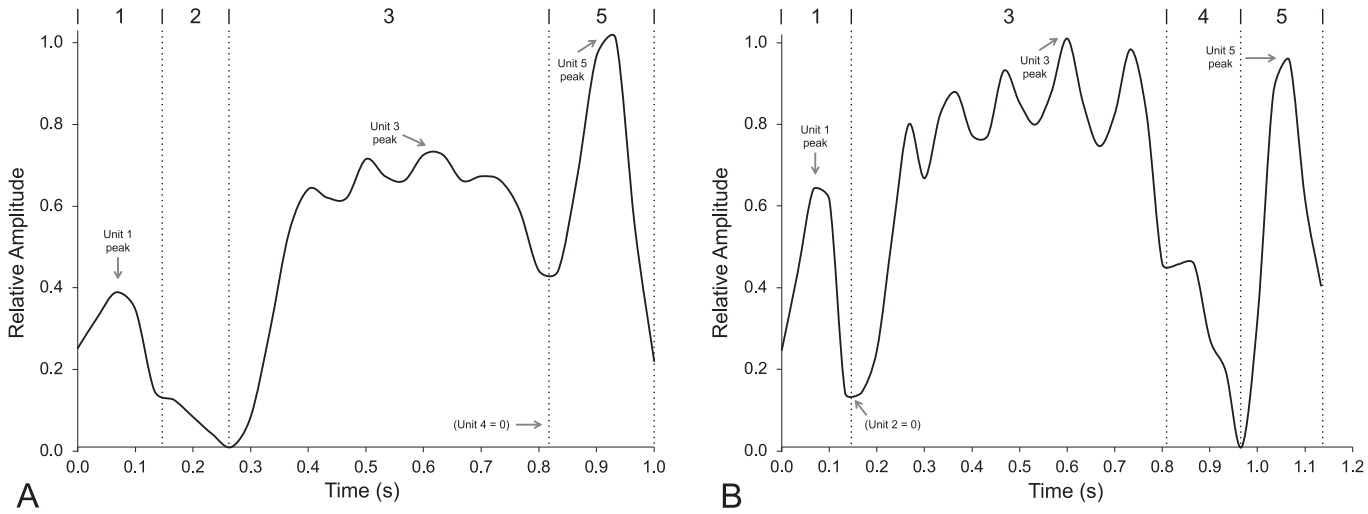

FIG. 1.—Example *M. bivittatus* signature displays from two adult males illustrating variation in unit durations, standardized peak amplitudes, and number of bob peaks in Unit 3.

Measurement of Display Structure

We divided the signature display of *M. bivittatus* into five units, where Units 1, 3, and 5 contain bobs and Units 2 and 4 are pauses between bobs (Fig. 1). Following Macedonia et al. (2019), for each display, we measured display duration, each unit's duration, and the amplitude of the highest bob in each of Units 1, 3, and 5. To obtain amplitude values, each display was standardized to a scale of 0–1 (Fig. 1). The standardization was achieved by subtracting the smallest y-axis value (i.e., vertical head motion) from every other value in the display, followed by dividing each resulting value by the largest y-axis value in the display. This process ensured that all bobbing displays would be measured on the same scale regardless of their distance from the video camera when recorded.

As a second approach to quantify bobbing display structure, we chose the Fourier transform, which is a method that we have used in prior studies but that otherwise has been rarely used in research of reptile stereotypic motion. Some notable exceptions include Fleishman (1986), in which the fast Fourier transform (FFT) was used to explore the similarity between the movement of wind-blown vegetation and the cryptic forward motion of the vine snake (*Oxybelis aeneus*), which feeds primarily on *Anolis* lizards (Fleishman 1985). In a later study, Fleishman (1988) used FFT to examine the relationship between the smooth sinusoidal motion of vegetation oscillating in the wind and the contrasting square wave motion of *Anolis auratus* bobbing displays. Previously, we have used the Fourier transform to extract 13 variables (Table 1) from bobbing displays of *Microlophus* sp. (Macedonia et al. 2019) and *Anolis* sp. (Macedonia et al. 2021). As in those studies, for each display, we use FFT to compute the discrete Fourier transform (DFT) in MATLAB (vR2016b; MathWorks®, Natick, MA). The DFT divides each display into a series of sinusoidal waves varying in frequency and amplitude, of which the sum recreates the original display. Our amplitude threshold was reduced to 75% of the mean amplitude to exclude spurious noise. A comparison of reverse transforms ensured that noise filtering had not oversimplified displays and that they still contained their distinctive features. The variable most anticipated to distinguish population-specific bobbing display traits was principal frequency, as it describes the most prominent trigonometric function underlying display structure (see Macedonia 2019, 2021). Four additional variables that covered low (0–5 Hz), middle (5–10 Hz), and high (10–15 Hz) frequency ranges (i.e., 12 total variables) further characterized the display transforms (Table 1). As results from Macedonia et al. (2021) showed that neither the unit-based approach nor the DFT-based method was consistently superior in detecting display structure differences among taxa, we used both methods here.

TABLE 1.—Names and definitions of the 13 Fourier transform-based variables used to quantify signature displays in *Microlophus bivittatus*. Table after Macedonia et al. (2019).

Variable number	Variable	Description
1	Principal frequency	Frequency corresponding to peak amplitude
2	Peak frequency	Frequency corresponding to largest amplitude from 0 to 5 Hz
3	Partial sum	Partial sum of amplitudes from 0 to 5 Hz
4	Percentage of sum	Proportion of partial sum of amplitude to total sum amplitude from 0 to 5 Hz
5	Mean amplitude	Mean amplitude from 0 to 5 Hz
6–9	Peak frequency, partial sum, percentage of sum, mean amplitude 5–10 Hz	Same as Variables 2–5, but for 5–10 Hz
10–13	Peak frequency, partial sum, percentage of sum, mean amplitude 10–15 Hz	Same as Variables 2–5, but for 10–15 Hz

Analysis of Display Structure

Our analytical approach follows a sequence of procedures like those used in our recent comparative studies of bobbing display structure (Macedonia et al. 2015, 2019, 2021). First, for our nine unit-based variables, we used descriptive statistics to determine unit duration mean, range, coefficient of variation (CV), and percent duration (we forwent calculating descriptive statistics for our 13 DFT variables). An exploratory data analysis using Spearman rank correlation revealed that some of our unit-based variables were significantly correlated. We, therefore, restricted between-population tests of significance to mean unit durations (one value per subject), as durations of these five variables (Units 1–5) were uncorrelated with one another in each population (Supplemental Table S2, available online). Second, we used balanced nested ANOVAs to partition display variance into between-population, among-subject, and within-subject variance. The use of balanced nested ANOVAs allowed us to detect whether some variables were better than others at revealing variation at a given level (e.g., Decourcy and Jenssen 1994; Lovern et al. 1999; Macedonia and Clark 2003; Orrell and Jenssen 2003). Third, we used principal components analysis (PCA) to transform our unit-based and DFT variables into smaller sets of normally distributed, uncorrelated variables. The resulting principal components (PCs) were Varimax rotated to maximize their interpretability relative to the original variables. Finally, we entered the rotated PCs into a linear discriminant function analysis (DFA) to determine how accurately each display could be assigned to the correct population by the discriminant functions. In SPSS, DFA generates the following two versions of the analysis: an original analysis, in which all cases (i.e., bobbing displays) are used to create the discriminant functions, and a leave-one-out cross-validation analysis, in which all cases except the case being classified are used to create the functions. The cross-validation analysis, therefore, produces a more generalizable result.

We used our suite of methods (nested ANOVA, PCA, and DFA) for separate analyses of our unit-based variables and DFT variables. Analyses first were run using values from measurements of two displays per subject (32 cases per population) and then were run again using measurement means (16 cases per population). We conducted the mean value analyses to eliminate the possibility of autocorrelation effects that might occur when including more than one display per subject.

Nested ANOVAs were carried out using a purposed Excel spreadsheet (http://udel.edu/~mcdonald/statnested.html) from the Handbook of Biological Statistics (McDonald 2014). Our PCA and DFA analyses were conducted in SPSS (v21.0, IBM Inc., Armonk, NY). Correlations among variables were examined by creating correlation matrices in VassarStats (available at http://www.vassarstats.net) separately for our unit-based and DFT variables. For our two study populations, (1) correlations between variable pairs were tested for significance using Spearman rank correlation, (2) uncorrelated mean unit durations of displays were compared using Mann–Whitney U tests, and (3) DFA classification success was tested using 2×2 contingency tables with Fisher's exact test in Social Science Statistics (https://www.socscistatistics.com).

RESULTS

Body Size and Sexual Size Dimorphism

Across *M. bivittatus* populations, natural log-transformed SVL was larger in males than that in females ($F_{1,220} = 268.7$, $P < 0.0001$) and was larger in Isla Lobos lizards than that in lizards on San Cristóbal at Punta Carola and Playa Ochoa ($F_{2,220} = 139.4$, $P < 0.0001$ overall and in both contrasts of adjusted means). We found a significant sex by location interaction ($F_{2,220} = 139.4$, $P < 0.0001$) in which the mean natural log-transformed SVL was larger in both sexes on Isla Lobos than at Punta Carola and Playa Ochoa ($P < 0.0001$ in all four contrasts of adjusted means; Fig. 2).

Sexual size dimorphism indices (SDIs) revealed that males were, on average, 18% larger than females at both Punta Carola and Playa Ochoa and were 52% larger than females at Isla Lobos (Table 2). Our findings are consistent with Rensch's Rule, which states that SSD increases with size when males are larger than females (see Cox et al. 2003, 2007; and Roitberg 2007 for reviews).

Bobbing Display Structure: Unit-Based Variables

As anticipated, descriptive statistics revealed strong similarities between the populations on San Cristóbal (Puerto Baquerizo Moreno) and Isla Lobos in our nine unit-based measures of bobbing displays. In both populations, bob unit durations (Units 1, 3, and 5) were stereotyped (CVs < 35%, Barlow 1977), whereas pause unit durations (Units 2 and 4) were more variable (Table 3). All bob unit peak amplitudes likewise were stereotyped, most notably Unit 5, for which the CV was less than 1% in the San Cristóbal population (Table 3). Results of Mann–Whitney U tests on uncorrelated mean unit durations (i.e., Units 1–5) revealed between-population differences in the following two units: Unit 1 was longer ($n = 16$, $U = 58$; $P = 0.009$) and Unit 4 was shorter ($n = 16$, $U = 65.5$; $P = 0.02$) in the Isla Lobos population than in the San Cristóbal population (Table 3).

Nested ANOVAs revealed that most variance in display unit durations and bob peak heights occurred within-subjects, followed by among-subject variation (Fig. 3a,b). However, two variables that were not significantly correlated in either population (Supplemental Table S2) accounted for a substantial amount of between-population variance, as follows: Unit 1 duration (26.33% of this variable's total variance, $F_{1,30} = 9.154$, $P = 0.005$; Fig. 3a) and Unit 5 peak amplitude (11.91% of this variable's total variance, $F_{1,30} = 4.702$, $P = 0.04$; Fig. 3b).

Individual measurements from two displays.—A PCA of unit-based variables, in which the measurements from two displays were entered for each subject, generated four PCs that accounted for roughly 79% of the data variance (Supplemental Table S3, available online). Rotated PC1 explained nearly 23% of that variance (Supplemental Table S3) and was most heavily weighted on display duration and Unit 1 duration (Supplemental Table S4, available online). A DFA on the four PCs generated a single function (Supplemental Table S5, available online) that was most heavily weighted on PC3 (which itself was most strongly influenced by Unit 1 peak amplitude) followed by PC1 (Supplemental Tables S4, S5). Thus, both attributes of Unit 1—duration in PC1 and peak amplitude in PC3—were particularly important in the DFA. Classification success was moderate for

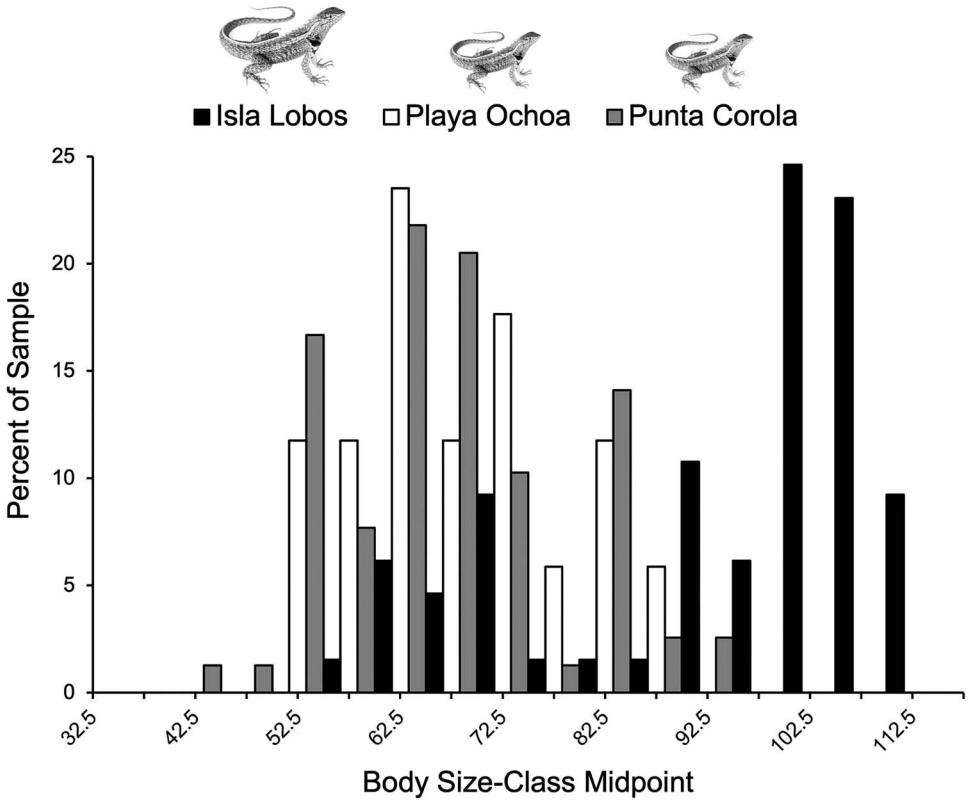

FIG. 2.—Body size distributions (SVLs measured in 1 mm increments) of male *M. bivittatus* samples. SVLs were binned in size classes of 5-mm intervals and are shown as the percentage of individuals for each study site. For example, the x-axis value 52.5 mm is the midpoint of the bin that contains SVLs from 50 mm to 55 mm. Playa Ochoa and Punta Carola are both located in southwestern San Cristóbal (see text for details of the study areas' geographical relationships). Above the name of each study location is an image of an adult male *M. bivittatus* (from Arteaga et al. 2019, with permission) that is scaled in size relative to the male mean SVL measurement for each population shown in Table 2.

both populations, with approximately 72% correct classification of 32 displays from San Cristóbal subjects and about 66% correct classification of 32 displays from Isla Lobos subjects (Table 4). The ability of the DFA to classify displays to the correct population differed from random assignment (Fisher's exact test, $P = 0.005$). In the cross-validation analysis, only two fewer cases were correctly classified to the San Cristóbal population (66%) than in the original analysis (72%) and 66% of cases again were correctly assigned to the Isla Lobos population (Fisher's exact test, $P = 0.02$; Table 4).

TABLE 2.—Mean ± SD (*n*) SVL and SDI for subjects at three study sites. SDI_1 = body size of larger sex/body size of smaller sex = (SVL_{male}/SVL_{female}) where male size-biased SSD arbitrarily receives a negative sign[a], and $SDI_2 = -(SVL_{male}/SVL_{female}) + 1$, where the SDI_2 value is centralized around a mean of zero[b]. We excluded the lower 25th percentile (defined by the smallest SVL value for which we observed reproductively active males and females) within each sex at each locality, thereby minimizing the inclusion of juveniles at each location. Playa Ochoa and Punta Carola are both located in southwestern San Cristóbal (see text for distances among study sites).

Location	Sex	SVL (*n*)	SDI_1, SDI_2
Isla Lobos	Female	65.30 ± 5.10 (37)	
	Male	98.97 ± 4.96 (34)	–1.52, –0.52
Playa Ochoa	Female	60.79 ± 4.68 (14)	
	Male	71.67 ± 8.89 (12)	–1.18, –0.18
Punta Carola	Female	59.56 ± 4.51 (70)	
	Male	70.09 ± 9.07 (58)	–1.18, –0.18

[a] Gibbons and Lovich (1990).
[b] Lovich and Gibbons (1992).

Measurement means from two displays.—When we used a mean value for each unit-based variable (averaged across each subject's two displays), a PCA generated four components that explained over 81% of the data variance. PC1 accounted for 25% of that variance (Supplemental Table S6, available online), where Display duration and Unit 1 duration again were heavily weighted, along with Unit 2 duration (Supplemental Table S7, available online). In a DFA on the four PCs, PC2 (primarily influenced by the peak amplitudes of Units 1 and 5) was the strongest component in the discriminant function, followed by PC1 (Supplemental Tables S7, S8). In both the original and cross-validation analyses, DFA correctly classified 75% of the San Cristóbal displays and 69% of the Isla Lobos displays—a result that differed from a random assignment of displays to population (Fisher's exact test, $P = 0.03$; Table 5). Thus, whether we used measurements from both displays of each subject or used each variable's mean value, DFA correctly predicted the population from which displays originated from 66% to 75% of the time.

Bobbing Display Structure: Fourier Transform-Based Variables

As with our unit-based variables, nested ANOVAs on 13 DFT variables revealed within-subject variance to be largest, followed by among-subject variance, and finally by between-population variance (Fig. 3c). However, the following two uncorrelated DFT variables (Supplemental Table S9, available

TABLE 3.—Between-population comparisons of bobbing displays from 16 males on the San Cristóbal mainland and 16 males on the adjacent islet of Isla Lobos. Each subject contributed a single mean value per parameter. Unit durations (Dur) in seconds. Unit Peak is an abbreviation for standardized peak amplitude (see text). Percent duration (% Dur) is a unit's mean duration as a proportion of all five unit's mean durations, which together sum to 100%. CV (%) = coefficient of variation. CVs with values of <35% meet Barlow's (1977) criterion of highly stereotyped behavior patterns.

	San Cristóbal				Isla Lobos			
Unit	Mean	Range	CV (%)	% Dur	Mean	Range	CV (%)	% Dur
U1 Dur	0.150	0.100–0.217	23.52	13.70	0.184	0.117–0.317	29.99	17.22
U2 Dur	0.092	0.033–0.200	50.27	9.54	0.150	0.000–0.500	69.07	13.67
U3 Dur	0.592	0.467–0.834	15.75	55.60	0.567	0.351–0.750	16.06	49.66
U4 Dur	0.033	0.000–0.100	78.35	3.69	0.000	0.000–0.300	166.60	1.55
U5 Dur	0.184	0.134–0.217	10.94	17.49	0.200	0.150–0.267	15.90	17.90
U1–5 Dur	1.075	0.834–1.317	12.12	—	1.150	0.900–1.567	14.05	—
U1 Peak	0.521	0.362–0.780	24.52	—	0.609	0.278–1.000	34.22	—
U3 Peak	0.744	0.664–0.978	12.94	—	0.818	0.544–0.963	14.15	—
U5 Peak	1.000	0.974–1.000	0.90	—	1.000	0.775–1.000	7.46	—

online) exhibited considerable between-population differences: low peak frequency (14.67% of this variable's total variance, $F_{1,30} = 5.434$; $P = 0.03$) and low frequency percentage of sum (24.32% of this variable's total variance, $F_{1,30} = 7.865$; $P = 0.009$; Fig. 3c).

Individual measurements from two displays.—A PCA of measurements from two displays of each subject produced five PCs. These five components explained nearly 85% of the total display variance (Supplemental Table S10, available online). PC1, which accounted for over 23% of that variance, was most strongly weighted on three of our four high-frequency variables (Supplemental Tables S10, S11, available online). A DFA on the five PCs produced a single discriminant function (Supplemental Table S12, available online) that correctly classified roughly 66% of displays to the correct population (Fisher's exact test, $P = 0.02$; Table 6). In the cross-validated analysis, about 64% of displays were correctly classified (Fisher's exact test, $P = 0.04$; Table 6). In contrast to our results for unit-based variables, outcomes of these two DFAs were biased in favor of Isla Lobos displays (72–75% correct classification) over those from San Cristóbal subjects (56.3% correct classification; Table 6).

Measurement means from two displays.—Finally, a PCA of DFT measurements averaged across subjects' two displays produced four PCs (Supplemental Table S13, available online). Together, these components accounted for about 79% of bobbing display variance, with PC1 and PC2 independently explaining nearly 24% of that variation each (Supplemental Table S13). As in the analysis where DFT measures from both of subjects' displays were used, three of our four high-frequency variables again were heavily weighted on PC1 (Supplemental Table S14, available online). A DFA on the four PCs produced a single function (Supplemental Table S15, available online) that was most strongly influenced by PC2, which itself was heavily weighted on principal frequency and a mix of low- and mid-frequency variables (Supplemental Table S14). This discriminant function assigned displays to the correct population 75% of the time in the original analysis (Fisher's exact test, $P = 0.01$; Table 7), without population bias. The cross-validated analysis was less successful than the original, however, with displays being assigned to the correct population about 66% of the time (Fisher's exact test, $P = 0.16$; Table 7). In summary, by using measurements from both displays of subjects, we found that DFA assigned approximately 56–75% of displays to the correct population, whereas when using mean values of each DFT measure, DFA was slightly more successful in classifying approximately 63–75% of displays to the correct population.

DISCUSSION

In this study, we have shown that the separation of two *M. bivittatus* populations over a brief period of geological time has resulted in population divergence in body size and SSD and has produced detectable population-level differences in bobbing display structure. Although we do not know the underlying mechanism(s) responsible for Isla Lobos male gigantism, several explanations seem possible. Ecological release (Herrmann et al. 2021) could play a role via (1) reduced between-sex competition for arthropod prey from increased SSD (see Stamps et al. 1997 for a review) or (2) reduced predation pressure from the San Cristóbal racer (*Pseudalsophis biserialis*)—a diurnal visually hunting snake that commonly preys on *Microlophus* sp. (Ortiz-Catedral et al. 2019). Meta-analyses of lizard body sizes from mainland (or large island) and small island populations suggest that both reduced predation pressure and increased food availability may favor larger body sizes in many island populations (Meiri 2007, 2008). If mortality from predation is lower in *M. bivittatus* on Isla Lobos than on San Cristóbal and individuals survive longer on Isla Lobos, we would anticipate larger body sizes in both sexes, which our data support (Table 2). A larger body size might, in turn, reduce predation success. Yet, relaxed predation pressure alone seems insufficient to explain large body size in Isla Lobos *M. bivittatus*. For example, the San Cristóbal racer was observed to be abundant on Isla Lobos in summer 2022, and an individual was video-recorded preying on an adult male *M. bivittatus* (C.A. Valle, personal observation). At present, we do not know if the high population density of the San Cristóbal racer is rare, common, or cyclic (seasonally or otherwise). It likewise is unknown if food availability or diet differs between San Cristóbal and Isla Lobos *M. bivittatus* populations.

Predation pressure and food availability also seem unlikely to explain the extreme SSD in Isla Lobos *M. bivittatus*. Rather, the limited space on Isla Lobos may favor large male body size in competition for and defense of territories that attract breeding females (Case 1982; Stamps et al. 1997; Jenssen et al. 2005; but see Lappin and Husak 2005). Ultimately, gigantism in Isla Lobos males could arise during development from higher levels of circulating testosterone and faster growth rates than in San Cristóbal males, as has been shown for some other lizard taxa (for reviews see Cox et al. 2007; John-Alder and Cox 2007).

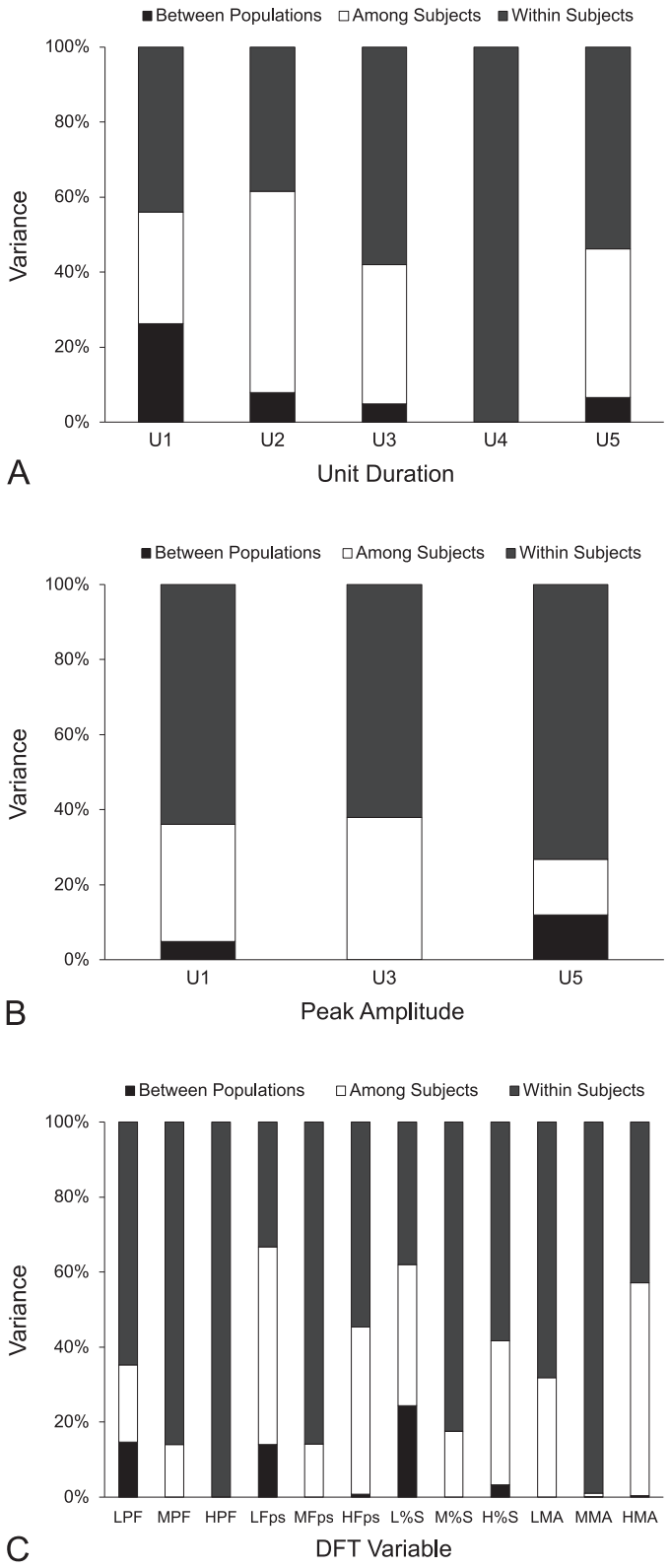

FIG. 3.—Stacked bar charts illustrating the sources and proportions of bobbing display variance in *Microlophus bivittatus* signature displays, as revealed in nested ANOVAs. For each variable, the three sources of variance (between populations, among subjects, and within subjects) add to 100%. Populations include 16 adult males from San Cristóbal (mainland) and 16 adult males from Isla Lobos. (A) Proportions of variance attributable to display unit durations in the five units (bobs and pauses) of signature displays. (B) Proportions of variance attributable to standardized peak amplitudes in the three bob units (Units 1, 3, and 5) of signature displays. (C) Proportions of variance attributable to 12 of 13 DFT variables measured for signature displays. Principal frequency results are not shown, as they were highly redundant with low peak frequency. Frequency ranges: low = 0–5 Hz, middle = 5–10 Hz, high = 10–15 Hz. Abbreviations: LPF = low peak frequency, MPF = middle peak frequency, HPF = high peak frequency, LFps = low frequency partial sum, MFps = middle frequency partial sum, HFps = high frequency partial sum, L%S = low frequency percentage of sum, M%S = middle frequency percentage of sum, H%S = high frequency percentage of sum, LMA = low frequency mean amplitude, MMA = middle frequency mean amplitude, and HMA = high frequency mean amplitude.

Summary of Population Differences in *M. bivittatus* Bobbing Display Structure

A significantly longer Unit 1 duration in the Isla Lobos population supported our hypothesis that displays would be performed more slowly than in the San Cristóbal population. Yet, Unit 4 duration (a pause between bobs) ran counter to our hypothesis, and durations of units 2, 3, and 5 did not differ between populations. Thus, on the whole, we did not find the inverse scaling of body size and display speed that we had predicted.

Nested ANOVA revealed substantial between-population variance in Unit 1 duration which, together with display duration, was of primary importance in our unit-based DFAs. Whether we used a measurement value for each variable from both displays of subjects (32 displays per population) or used mean values from each subject's two displays (16 displays per population), DFA assigned displays to the correct population at a level significantly greater than random chance in every analysis.

Similar to our results with unit-based measures, nested ANOVAs showed that most variance in DFT variables fell within and among subjects. Yet, between-subject values for two variables, low peak frequency and low frequency percentage of sum, differed significantly between populations. Although it is unclear why DFA was biased in correctly classifying displays to the Isla Lobos population when values from both displays of subjects were used (Table 6), in all but one comparison (i.e., cross-validation; Table 7) our DFAs assigned displays to the correct population at a level significantly greater than chance. Taken together, we find these results remarkable, given the very close geographic proximity of the two islands and the short amount of time that the two populations have been diverged (almost certainly < 5 kyr).

Sexual Size Dimorphism (SSD) and Display Repertoire Size

Like most other territorial lizard taxa, *Microlophus* sp. exhibits a variety of nonbobbing displays and postures in the contexts of courtship and territory defense. Although the focus of the present study is on bobbing display structure, in a prior study (Clark et al. 2023) we analyzed nonbobbing displays in comparing subjects' responses to the manipulation of shoulder epaulets (a potentially sexually selected ornament; see below) in robotic conspecifics. Seven types of nonbobbing displays (termed "display modifiers" by Jenssen 1977, 1978) were observed and comprised an additive composite response score that we calculated for our Puerto Baquerizo Moreno subjects (Clark et al. 2023). Previously, it has been argued for the Iguania that nonbobbing display diversity determines lizard display repertoire complexity and that complexity is positively correlated with male-biased

TABLE 4.—Discriminant function analysis of four PCs derived from six unit duration variables and three standardized peak amplitude variables measured in bobbing displays of two *Microlophus bivittatus* populations. In this analysis, 16 males from each population contributed 2 values (one from each display) for each of the 9 variables measured in their 2 displays. Data were analyzed as a 2 × 2 contingency table with Fisher's exact test. In the cross-validated analysis, each case was classified by the function(s) derived from all cases other than that case. Number and percentage of correct display assignments are in bold text.

	Predicted group membership			
	San Cristóbal	Isla Lobos	Total	*P* value
Original analysis[a]				
Population				
San Cristóbal	**23 (71.9%)**	9 (28.1%)	32 (100%)	
Isla Lobos	11 (34.4%)	**21 (65.6%)**	32 (100%)	0.01
Cross-validated[b]				
Population				
San Cristóbal	**21 (65.6%)**	11 (34.4%)	32 (100%)	
Isla Lobos	11 (34.4%)	**21 (65.6%)**	32 (100%)	0.02

[a] 68.8% of cases in the original analysis were classified correctly to population.
[b] 65.6% of cross-validated cases were classified correctly to population.

SSD (Ord et al. 2001). As male-biased SSD in lizards often gives large males a mating advantage over small males (Cox et al. 2003), it seems possible that extreme SSD in Isla Lobos *M. bivittatus* males might have favored greater diversity in nonbobbing display types (complexity) not observed on San Cristóbal. Although purely speculative, this prediction is testable.

Sexual Size Dimorphism (SSD) and Ornament Size

Intense sexual selection may result in exaggerated morphological signals in large males (positive or hyperallometry) that may render them more attractive to females (Summers and Ord 2022). One possible driver for the evolution of supersized *M. bivittatus* males on Isla Lobos is that increased shoulder epaulet size—an ornament exclusive to males—is commensurate with increased body size. Previously, we have shown that male subjects on San Cristóbal accumulated significantly larger composite response scores (i.e., greater diversity of display modifiers in a trial) in response to an enlarged (approximately 200% of average) black shoulder epaulet on male conspecific robots as compared to a reduced (approximately 50% of average) epaulet on the robot's opposite side (see Clark et al. 2023: their Figs. 1 and 6). This manipulation bears repeating as an interpopulation experiment on San Cristóbal and Isla Lobos. In light of the extreme SSD of *M. bivittatus* on Isla Lobos, we would predict exceptionally strong responses of Isla Lobos males to enlarged shoulder epaulets, as compared to epaulets reduced in size.

TABLE 5.—Discriminant function analysis of four PCs derived from our nine unit-based variables measured in bobbing displays of two *M. bivittatus* populations. In this analysis, 16 males from each population contributed one mean value for each of the 9 variables measured in their 2 displays. Legend as in Table 4.

Original analysis and cross-validated[a] Population	Predicted group membership			
	San Cristóbal	Isla Lobos	Total	*P* value
San Cristóbal	**12 (75.0%)**	4 (25.0%)	16 (100%)	
Isla Lobos	5 (31.3%)	**11 (68.8%)**	16 (100%)	0.03

[a] Results of the original and cross-validated analyses were identical. In both analyses, 71.9% of cases were classified correctly to population in the same manner.

TABLE 6.—Discriminant function analysis of 5 principal components derived from 13 DFT variables measured in bobbing displays from 2 populations of *Microlophus bivittatus*. In this analysis, 16 males from each study population contributed 2 values (1 from each display) for each of the variables measured in their 2 displays. Legend as in Table 4.

	Predicted group membership			
	San Cristóbal	Isla Lobos	Total	*P* value
Original analysis[a]				
Population				
San Cristóbal	**18 (56.3%)**	14 (43.7%)	32 (100%)	
Isla Lobos	8 (25.0%)	**24 (75.0%)**	32 (100%)	0.02
Cross-validated[b]				
Population				
San Cristóbal	**18 (56.3%)**	14 (43.7%)	32 (100%)	
Isla Lobos	9 (28.1%)	**23 (71.9%)**	32 (100%)	0.04

[a] 65.5% of cases in the original analysis were classified correctly to population.
[b] 64.1% of cross-validated cases were classified correctly to population.

Bobbing Display Structure Divergence: Comparisons with *Anolis* and Future Directions

In several previous studies of the large lizard genus *Anolis*, geographically disjunct conspecific populations as well as geographically adjacent cryptic (sibling) species have been shown to differ in bobbing display structure (e.g., Garcia and Gorman 1968). Below we summarize two of those studies and ask how their findings compare with results from our present work. We then propose future research that could address some of the gaps in our knowledge of display divergence in Lava Lizard populations.

First, Jenssen (1981) found that although *Anolis grahami grahami* from southeast (Kingston) and central (Mandeville) Jamaica exhibited the same bobbing display structure, this structure differed considerably from that of conspecifics on the Jamaican West coast (Negril). Bobs in the Kingston and Mandeville populations were plateau shaped due to long pauses at the apices of the bobs, whereas those in the Negril population were spike shaped due to the absence of pauses during bobs. More recently, it was shown that a population of *A. g. grahami* on the northcentral coast of Jamaica (Discovery Bay), which lies longitudinally between Kingston and Negril, performed displays with bob morphology intermediate between plateau shaped and spike shaped (i.e., flat-topped spikes, Macedonia et al. 2021: their Fig. 4). Interestingly, chromosome number in *A. g. grahami* covaries with bob structure along an

TABLE 7.—Discriminant function analysis of 4 principal components derived from 13 DFT variables measured in bobbing displays from two populations of *Microlophus bivittatus*. In this analysis, 16 males from each study population contributed 1 mean value for each of the variables measured in their 2 displays. Legend as in Table 4.

	Predicted group membership			
	San Cristóbal	Isla Lobos	Total	*P*
Original analysis[a]				
Population				
San Cristóbal	**12 (75.0%)**	4 (25.0%)	16 (100%)	
Isla Lobos	4 (25.0%)	**12 (75.0%)**	16 (100%)	0.01
Cross-validated[b]				
Population				
San Cristóbal	**10 (62.5%)**	6 (37.5%)	16 (100%)	
Isla Lobos	5 (31.3%)	**11 (68.8%)**	16 (100%)	0.16

[a] 75.0% of cases in the original analysis were classified correctly to population.
[b] 65.6% of cross-validated cases were classified correctly to population.

east–west longitudinal transect, as follows: (1) Kingston, plateau-shaped bobs and 2n = 32; (2) Discovery Bay, flat-topped, spike-shaped bobs and 2n = 34; and (3) Negril, spike-shaped bobs and 2n = 36 (see Macedonia et al. 2021). It seems possible that at least some of these populations may be sibling species. Notably, it has yet to be examined if display structure experiences character displacement where these genetically distinct *A. g. grahami* populations come into secondary contact in Jamaica.

As a second example, Jenssen and Gladson (1984) investigated bobbing displays in three Haitian sibling species of the *Anolis brevirostris* complex (once considered conspecifics). They found the largest differences in display structure at the intersection of two species' distributions, namely, *Anolis websteri* at Montrouis and *Anolis caudalis* at Trou Forban. This finding mirrored genetic and dewlap color differences, where males at Montrouis possessed bright orange dewlaps but those in nearby Trou Forban exhibited pale, yellowish-white dewlaps (Webster and Burns 1973; Lambert et al. 2013). The authors of these studies have argued that the patterns of display variation (motion and color) and genetic differentiation support the hypothesis of character displacement via reinforcement, where differences are most pronounced in secondary contact.

Although other comparisons of *Anolis* bobbing display structure at the population level exist (e.g., Lovern et al. 1999; Macedonia and Clark 2001, 2003; Macedonia et al. 2015), how do the summarized examples above inform the findings of the present study and frame questions for future research? First, the work on *A. g. grahami* in Jamaica suggests a generalizable relationship between the geographic distance of populations and the degree of display structure divergence. As our bobbing display data for *M. bivittatus* on San Cristóbal originate from one sampling area, a test that compares display structure covariation with geographic distance currently is not possible. Ideally, such tests would use populations on San Cristóbal for which we already have morphometric and genetic data (see below).

Likewise, results of multiple studies have supported the argument that, due to reproductive reinforcement, Haitian populations of *Anolis* sibling species in secondary contact (*A. websteri* and *A. caudalis*) exhibit greater display structure divergence than populations of the same two sibling species somewhat further from each other. Although *A. bivittatus* is allopatric with all other *Microlophus* species, we do not yet know if reproductive reinforcement has occurred between any populations that have been isolated on San Cristóbal for a period of geological time but that now are in secondary contact. Nevertheless, our bobbing display data from two *M. bivittatus* populations that are approximately 10 km apart (Puerto Baquerizo Moreno and Isla Lobos) offer a starting point for among-population comparisons of display structure. Importantly, microsatellite data have shown that pairwise genetic differences (F_{ST}) between populations sampled on Isla Lobos and four San Cristóbal locations range from 0.021 to 0.194, with a difference of 0.135 between subjects on Isla Lobos and those at Puerto Baquerizo Moreno where we recorded lizard displays (A.M. Troya Zuleta and C.A. Valle, personal observations). These genetic data provide an opportunity to determine how closely display structure differences reflect genetic differences among *M. bivittatus* populations, in a manner similar to *Anolis* research in Jamaica and Haiti.

Finally, the distributions of numerous species pairs of *Microlophus* overlap or abut on the western edge of South America (for distribution maps see Toyama and Boccia 2022), including three species for which bobbing display structure is known (Clark et al. 2015). Thus, the Galápagos Islands and coastal South America offer fertile ground for future research on genetic differentiation and bobbing display structure divergence in *Microlophus*.

Acknowledgments.—We thank J.P. Muñoz, Administrador e Investigador, and S. Sotamba of the Galápagos Science Center (San Cristóbal). We are grateful to the Parque Nacional Galápagos Ecuador, San Cristóbal, for their support and permission to conduct research on Galápagos Lava Lizards (Research Permit: PC-68-21 #162). R. Clark and K. Stricker were fundamental in the production and appearance of the lizard models used as display-eliciting stimuli. All contributors to this study observed ethical and legal guidelines and regulations as specified in the ASIH-HL-SSAR Guidelines for Use of Live Amphibians and Reptiles in Field Research. No animals were collected for this study. Supplements available at https://www.macedonialab.com/publications.

Supplemental Material

Supplemental material associated with this article can be found online at https://doi.org/10.1655/Herpetologica-D-23-00011.s1, https://doi.org/10.1655/Herpetologica-D-23-00011.s2, https://doi.org/10.1655/Herpetologica-D-23-00011.s3, https://doi.org/10.1655/Herpetologica-D-23-00011.s4, https://doi.org/10.1655/Herpetologica-D-23-00011.s5, https://doi.org/10.1655/Herpetologica-D-23-00011.s6, and https://doi.org/10.1655/Herpetologica-D-23-00011.s7.

Literature Cited

Ali, J.R., and J.C. Aitchison. 2014. Exploring the combined role of eustasy and oceanic island thermal subsidence in shaping biodiversity on the Galápagos. Journal of Biogeography 41:1227–1241.

Allen, W.L., M. Stevens, and J.P. Higham. 2014. Character displacement of Cercopithecini primate visual signals. Nature Communications 5:1–10.

Arteaga, A., L. Bustamante, J. Viera, W. Tapia, and J.M. Guayasamin. 2019. Reptiles of the Galápagos: Life on the Enchanted Islands. Available at https://www.reptilesofecuador.com/microlophus_bivittatus.html. Tropical Herping, Ecuador.

Barlow, G.W. 1977. Modal action patterns. Pp. 98–134 in How Animals Communicate (T.A. Sebeok, ed.). Indiana University Press, USA.

Benavides, E., R. Baum, H.M. Snell, H.L. Snell, and J.W. Sites. 2009. Island biogeography of the Galápagos lava lizards (Tropiduridae: *Microlophus*): Species diversity and colonization of the archipelago. Evolution 63:1606–1626.

Bradbury, J.W., and S.L. Vehrencamp. 2011. Principles of Animal Communication, 2nd edition. Sinauer Associates, Inc., USA.

Brown, D., W. Christian, and R.M. Hanson. 2021. Tracker Video Analysis and Modeling Tool, Version 6.0.1. Available at https://physlets.org/tracker. Open source software, publicly available under the GNU General Public License Version 3.

Carpenter, C.C. 1966. Comparative behavior of the Galápagos lava lizards (*Tropidurus*). Pp. 269–273 in The Galápagos: Proceedings of the Galápagos International Scientific Project (R.I. Bowman, ed.). University of California Press, USA.

Carpenter, C.C., and G.G. Grubitz, III. 1961. Time-motion study of a lizard. Ecology 42:199–200.

Case, T.J. 1982. Ecology and evolution of the insular giant chuckwallas, *Sauromalus hispidus* and *Sauromalis varius*. Pp. 184–212 in Iguanas of the World: Their Behaviour, Ecology and Conservation (G.M. Burghardt and A.S. Rand, eds.). Noyes Publications, USA.

Clark, D.L., J.M. Macedonia, J.W. Rowe, M.A. Stuart, D.J. Kemp, and T.J. Ord. 2015. Evolution of displays in Galápagos lava lizards: Comparative analyses of signalers and robot playbacks to receivers. Animal Behaviour 109:33–34.

Clark, D.L., J.M. Macedonia, J.C. Gillingham, J.W. Rowe, H.J. Kane, and C.A. Valle. 2016. Why does conspecific display recognition differ among species of Galápagos lava lizards? A test using lizard robots. Herpetologica 72:47–54.

Clark, D.L., J.M. Macedonia, J.W. Rowe, K. Kamp, and C.A. Valle. 2017. Responses of Galápagos lava lizards (*Microlophus bivittatus*) to manipulation of female nuptial coloration on lizard robots. Herpetologica 73:323–330.

Clark, D.L., J.M. Macedonia, J.W. Rowe, M.R. Austin, I.M. Centurione, and C.A. Valle. 2019. Galápagos lava lizards (*Microlophus bivittatus*) respond dynamically to displays from interactive conspecific robots. Behavioral Ecology and Sociobiology 76:136.

Clark, D.L., J.M. Macedonia, E.E. Neyer, A.M.E. Mish, J.W. Rowe, and C.A. Valle. 2023. Display responses of Galápagos lava lizards (*Microlophus bivittatus*) to manipulation of male shoulder epaulets in conspecific-mimicking robots. Herpetologica 79:37–47.

Cox, R.M., S.L. Skelly, and H.B. John-Alder. 2003. A comparative test of adaptive hypotheses for sexual size dimorphism in lizards. Evolution 57:1653–1669.

Cox, R.M., M.A. Butler, and H.B. John-Alder. 2007. The evolution of sexual size dimorphism in reptiles. Pp. 38–49 in Sex, Size, and Gender Roles: Evolutionary Studies of Sexual Size Dimorphism (D.J. Fairbairn, W.U. Blanckenhorn and T. Székely, eds.). Oxford University Press, UK.

Cummings, M.E., and L.R. Crothers. 2013. Interacting selection diversifies warning signals in a polytypic frog: An examination with the strawberry poison frog. Evolutionary Ecology 27:693–710.

Darwin, C. 1871. The Decent of Man in Relation to Sex. Murray, UK.

Decourcy, K.R., and T.A. Jenssen. 1994. Structure and use of male territorial headbob signals by the lizard *Anolis carolinensis*. Animal Behaviour 47:251–262.

Dial, K.P., E. Greene, and D.J. Irschick. 2008. Allometry of behavior. Trends in Ecology and Evolution 23:394–401.

Eilas, D.O., E.A. Hebets, R.R. Hoy, W.P. Madison, and A.C. Mason. 2006. Regional seismic song differences in sky island populations of the jumping spider, *Habronattus pugillis* Griswold (Araneae, Salticidae). The Journal of Arachnology 34:454–556.

Eliason, C.M. 2018. How do complex animal signals evolve? PLOS Biology 16:e3000093.

Fleishman, L.J. 1985. Cryptic movement in the vine snake *Oxybelis aeneus*. Copeia 1985:242–245.

Fleishman, L.J. 1986. Motion detection in the presence and absence of background motion in an *Anolis* lizard. Journal of Comparative Physiology A 159:711–720.

Fleishman, L.J. 1988. Sensory and environmental influences on display form in *Anolis auratus*, a grass anole from Panama. Behavioral Ecology and Sociobiology 22:309–316.

Garcia, R., and G. Gorman. 1968. Difference in male territorial display behavior in two sibling species of *Anolis*. Copeia 1968:419–420.

Gehara, M., K. Summers, and J.L. Brown. 2013. Population expansion, isolation and selection: Novel insights on the evolution of color diversity in the strawberry poison frog. Evolutionary Ecology 27:797–824.

Gibbons, J.W., and J.E. Lovich. 1990. Sexual dimorphism in turtles with emphasis on the slider turtle (*Trachemys scripta*). Herpetological Monographs 4:1–29.

Girard, M.B., D.O. Elias, G. Azevedo, K. Bi, M.M. Kasumovic, J.M. Waldock, E.B. Rosenblum, and M. Hedin. 2021. Phylogenomics of peacock spiders and their kin (Salticidae: *Maratus*), with implications for the evolution of male courtship displays. Biological Journal of the Linnean Society 132:474–494.

Guillory, W.X., M.R. Muell, K. Summers, and J.L. Brown. 2019. Phylogenomic reconstruction of the neotropical poison frogs (Dendrobatidae) and their conservation. Diversity 11:126.

Herrmann, N.C., J.T. Stroud, and J.B. Losos. 2021. Evolution of "ecological release" into the 21st century. Trends in Ecology and Evolution 36:206–215.

Irestedt, M., K.A. Jønsson, J. Fjeldså, L. Christidis, and P.G.P. Ericson. 2009. An unexpectedly long history of sexual selection in birds-of-paradise. BMC Evolutionary Biology 9:235.

Jenssen, T.A. 1977. Evolution of anoline lizard display behavior. American Zoologist 17:203–215.

Jenssen, T.A. 1978. Display diversity in anoline lizards and problems of interpretation. Pp. 269–285 in Behavior and Neurology of Lizards: An Interdisciplinary Conference (N. Greenberg and P.D. MacLean, eds.). National Institute of Mental Health, USA.

Jenssen, T.A. 1981. Unusual display behavior by *Anolis grahami* from western Jamaica. Copeia 1981:728–733.

Jenssen, T.A., and N.L. Gladson. 1984. Comparative display analysis of the *Anolis brevirostris* complex in Haiti. Journal of Herpetology 18:217–230.

Jenssen, T.A., K.R. Decourcy, and J.D. Congdon. 2005. Assessment in contests of male lizards (Anolis carolinensis): How should smaller males respond when size matters? Animal Behavior 69:1325–1336.

John-Alder, H.B., and R.M. Cox. 2007. Development of sexual size dimorphism in lizards: Testosterone as a bipotential growth regulator. Pp. 195–204 in Sex, Size, and Gender Roles: Evolutionary Studies of Sexual Size Dimorphism (D.J. Fairbairn, W.U. Blanckenhorn, and T. Székely, eds.). Oxford University Press, UK.

Kronforst, M.R., and L.E. Gilbert. 2008. The population genetics of mimetic diversity in *Heliconius* butterflies. Proceedings of the Royal Society B 275:493–500.

Lambert, S.M., A.J. Geneva, D.L. Mahler, and R.E. Glor. 2013. Using genomic data to revisit an early example of reproductive character displacement in Haitian *Anolis* lizards. Molecular Ecology 22:3981–3995.

Lappin, A.K., and J.F. Husak. 2005. Weapon performance, not size, determines mating success and potential reproductive output in the collared lizard (*Crotaphytus collaris*). The American Naturalist 166:426–436.

Ligon, R.A., C.D. Diaz, J.L. Morano, J. Troscianko, M. Stevens, A. Moskeland, T. Laman, and E. Scholes, III. 2018. Evolution of correlated complexity in the radically different courtship signals of birds-of-paradise. PLOS Biology 16:e2006962.

Losos, J.B. 2009. Lizards in an Evolutionary Tree: Ecology and Adaptive Radiation of Anoles. University of California Press, USA.

Losos, J.B., T.R. Jackman, A. Larson, K. de Queiroz, and L. Rodríguez-Schettino. 1998. Contingency and determinism in replicated adaptive radiations of island lizards. Science 279:2115–2118.

Lovern, M.B., T.A. Jenssen, K.S. Orrell, and T. Tuchak. 1999. Comparisons of temporal display structure across contexts and populations in male *Anolis* carolinensis: Signal stability or lability? Herpetologica 55:222–234.

Lovich, J.E., and J.W. Gibbons. 1992. A review of techniques for quantifying sexual size dimorphism. Growth, Development, and Aging 56:269–281.

Mahler, D.L., L.J. Revell, R.E. Glor, and J.B. Losos. 2010. Ecological opportunity and the rate of morphological evolution in the diversification of Greater Antillean anoles. Evolution 64:2731–2745.

Mahler, D.L., T. Ingram, L.J. Revell, and J.B. Losos. 2013. Exceptional convergence on the macroevolutionary landscape of island lizard radiations. Science 341:292–295.

Macedonia, J.M., and D.L. Clark. 2001. Headbob display analysis of the Grand Cayman anole, *Anolis conspersus*. Journal of Herpetology 35:300–310.

Macedonia, J.M., and D.L. Clark. 2003. Headbob display structure in the naturalized *Anolis* lizards of Bermuda: Sex, context, and population effects. Journal of Herpetology 37:266–276.

Macedonia, J.M., D.L. Clark, L.E. Cherry, N.E. Mohamed, and B.W. Bartel. 2015. Comparison of headbob displays in gray-dewlapped and red-dewlapped populations of green anoles (*Anolis carolinensis*). Herpetologica 71:117–124.

Macedonia, J.M., D.L. Clark, M.R. Fonley, I. Centurione, J.W. Rowe, and C.A. Valle. 2019. Analysis of bobbing displays in four species of Galápagos lava lizards using conventional and novel quantitative methods. Herpetologica 74:290–300.

Macedonia, J.M., D.L. Clark, and M.R. Fonley. 2021. Analysis of bobbing displays in the *grahami* series of anoles from Jamaica and Grand Cayman. Herpetological Monographs 35:65–89.

Masta, S.E., and W.P. Maddison. 2002. Sexual selection driving diversification in jumping spiders. Proceedings of the National Academy of Sciences of the United States of America 99:4442–4447.

McDonald, J.H. 2014. Handbook of Biological Statistics, 3rd edition. Available at http://www.biostathandbook.com. Archived by WebCite at http://www.webcitation.org/6RgCVpl4x on 8 August 2014. Sparky House Publishing, USA.

Meiri, S. 2007. Size evolution in lizards. Global Ecology and Biogeography 16:702–708.

Meiri, S. 2008. Evolution and ecology of lizard body sizes. Global Ecology and Biogeography 17:724–734.

Ng, J., and R. Glor. 2011. Genetic differentiation among populations of a Hispaniolan trunk anole that exhibit geographical variation in dewlap color. Molecular Ecology 20:4302–4317.

Ng, J., A.J. Geneva, S. Noll, and R.E. Glor. 2017. Signals and speciation: Anolis dewlap color as a reproductive barrier. Journal of Herpetology 51:437–447.

Noonan, B.P., and P. Gaucher. 2006. Refugial isolation and secondary contact in the dyeing poison frog *Dendrobates tinctorius*. Molecular Ecology 15:4425–4435.

Ord, T.J., D.T. Blumstein, and C.S. Evans. 2001. Intrasexual selection predicts the evolution of signal complexity in lizards. Proceedings of the Royal Society B 268:737–744.

Orrell, K.S., and T.A. Jenssen. 2003. Heterosexual signalling by the lizard *Anolis carolinensis*, with intersexual comparisons across contexts. Behaviour 140:603–634.

Ortiz-Catedral, L., E. Christian, M.J.A. Skirrow, D. Rueda, C. Sevilla, K. Kumar, E.M.R. Reyes, and J.C. Daltry. 2019. Diet of six species of terrestrial snakes (*Pseudoalsophis* spp.) inferred from faecal samples. Herpetological Notes 12:701–704.

Poulos, S.E., G. Ghionis, and H. Maroukian. 2009. Sea-level rise trends in the Attico-Cycladic region (Aegean Sea) during the last 5000 years. Geomorphology 107:10–17.

Richards-Zawacki, C.L., and M.E. Cummings. 2014. Intraspecific reproductive character displacement in a polymorphic poison dart frog, *Dendrobates pumilio*. Evolution 65:259–267.

Roitberg, E.S. 2007. Variation in sexual size dimorphism within a widespread lizard species. Pp. 143–153 in Sex, Size, and Gender Roles: Evolutionary Studies of Sexual Size Dimorphism (D.J. Fairbairn, W.U. Blanckenhorn, and T. Székely, eds.). Oxford University Press, UK.

Rudh, A., B. Rogell, O. Håstad, and A. Qvarnström. 2011. Rapid population divergence linked with co-variation between coloration and sexual display in strawberry poison frogs. Evolution 65:1271–1282.

Siddiqui, A., T.W. Cronin, E.R. Loew, M. Vorobyev, and K. Summers. 2004. Interspecific and intraspecific views of color signals in the strawberry poison frog *Dendrobates pumilio*. The Journal of Experimental Biology 207:2471–2485.

Stamps, J.A., and G.W. Barlow. 1973. Variation and stereotypy in the displays of *Anolis aeneus* (Sauria: Iguanidae). Behaviour 47:67–94.

Stamps, J.A., J.B. Losos, and R.M. Andrews. 1997. A comparative study of population density and sexual size dimorphism in lizards. The American Naturalist 149:64–90.

Summers, T.C., and T.J. Ord. 2022. Female preference for super-sized male ornaments and its implications for the evolution of ornament allometry. Evolutionary Ecology 36:701–716.

Tinghitella, R.M., A.C.R. Lackey, M. Martin, P.D. Dijkstra, J.P. Drury, R. Heathcote, J. Keagy, E.S.C. Scordato, and A.M. Meyers. 2018. On the role of male competition in speciation: A review and research agenda. Behavioral Ecology 29:783–797.

Toyama, K.S., and C.K. Boccia. 2022. Bergmann's rule in *Microlophus* lizards: Testing for latitudinal and climatic gradients of body size. bioRxiv. https://dx.doi.org/10.1101/2022.01.18.476846.

Webster, T.P., and J.M. Burns. 1973. Dewlap color variation and electrophoretically detected sibling species in a Haitian lizard, *Anolis brevirostris*. Evolution 27:368–377.

Accepted on 10 September 2023
Published on 29 December 2023
Associate Editor: Ryan Taylor

TABLE S1.—Studies that have used Display Action Patterns (DAP) to graphically illustrate and (usually) quantify interspecific variation of bobbing display structure in lizard genera. Asterisks following citation years indicate studies in which intraspecific population divergence in bobbing displays has been documented.

Genus	Authors
Anolis	Ruibal 1967; Garcia and Gorman 1968; Gorman 1968; Echelle et al., 1971; Jenssen, 1971*, 1977, 1978, 1981*, 1983; Jenssen and Gladson 1984; Lovern et al. 1999*; Macedonia and Stamps 1994; Queral et al. 1995; Macedonia and Clark 2001*, 2003*; Macedonia et al. 2015*, 2019*, 2021*; Ord and Martins 2006; Ord et al. 2007, 2013; Nelson and Ord 2022*; Nelson et al. 2022*
Amphibolurus/ *Ctenophorus*	Carpenter et al. 1970; Gibbons 1979*; Ramos and Peters 2021
Cyclura	Martins and Lamont 1998*
Diporiphora	Peters et al., 2022
Liolaemus	Martins et al. 2004
Microlophus	Clark et al. 2015, 2016, 2019; Macedonia et al. 2019
Sceloporus	Ferguson 1973*; Carpenter 1978; Martins 1993; Ord and Martins 2006; Martins et al. 1998*, 2015
Urosaurus	Carpenter 1962
Uta	Ferguson 1971*; McKinney 1971

LITERATURE CITED IN TABLE S1

Carpenter, C.C. 1962. A comparison of the pattern of display in *Urosaurus*, *Uta*, and *Streptosaurus*. Herpetologica 18:145-152.

Carpenter, C.C. 1978. Comparative display behavior in the genus *Sceloporus* (Iguanidae). Contributions in Biology and Geology to the Milwaukee Public Museum 18:1–71.

Carpenter, C.C., J.A. Badham, and B. Kimball. 1970. Behavior patterns of three species of *Amphibolurus* (Agamidae). Copeia 1970:497–505.

Clark, D.L., J.M. Macedonia, J.W. Rowe, M.A. Stuart, D.J. Kemp, and T.J. Ord. 2015. Evolution of displays in Galápagos lava lizards: Comparative analyses of signalers and robot playbacks to receivers. Animal Behaviour 109:33–34.

Clark, D.L., J.M. Macedonia, J.C. Gillingham, J.W. Rowe, H.J. Kane, and C.A. Valle. 2016. Why does conspecific display recognition differ among species of Galápagos lava lizards? A test using lizard robots. Herpetologica 72:47–54.

Clark, D.L., J.M. Macedonia, J.W. Rowe, M.R. Austin, I.M. Centurione, and C.A. Valle. 2019. Galápagos lava lizards (*Microlophus bivittatus*) respond dynamically to displays from interactive conspecific robots. Behavioral Ecology and Sociobiology 76:136.

Echelle, A.A., A.F. Echelle, and H.S. Fitch. 1971. A comparative analysis of aggressive display in nine species of Costa Rican *Anolis*. Herpetologica 27:271–288.

Ferguson, G.W. 1971. Variation and evolution of the push-up displays of the side-blotched lizard genus *Uta* (Iguanidae). Systematic Zoology 20:79–101.

Ferguson, G.W. 1973. Character displacement of the push-up displays of two partially-sympatric species of spiny lizards, *Sceloporus* (Sauria: Iguanidae). Herpetologica 29:281–284.

Garcia, R., and G. Gorman. 1968. Difference in male territorial display behavior in two sibling species of *Anolis*. Copeia 1968:419–420.

Gibbons, J.R.H. 1979. The hind leg pushup display of the *Amphibolurus decresii* species complex (Lacertilia: Agamidae). Copeia 1979:29–40.

Gorman, G.C. 1968. The relationships of *Anolis* of the *roquet* species group (Sauria:Iguanidae) — III. Comparative study of display behavior. Breviora 284:1–31.

Jenssen, T.A. 1971. Display analysis of *Anolis nebulosus* (Sauria, Iguanidae). Copeia 1971:197–209.

Jenssen, T.A. 1977. Evolution of anoline lizard display behavior. American Zoologist 17:203–215.

Jenssen, T.A. 1978. Display diversity in anoline lizards and problems of interpretation. Pp. 269-285 in Behavior and Neurology of Lizards: An Interdisciplinary Conference (N. Greenberg and P.D. MacLean, eds.). N.I.M.H., USA.

Jenssen, T.A. 1981. Unusual display behavior by *Anolis grahami* from western Jamaica. Copeia 1981:728–733.

Jenssen, T.A. 1983. Display behavior of two Haitian lizards, *Anolis cybotes* and *Anolis distichus*. Pp. 552–569 in Advances in Herpetology and Evolutionary Biology: Essays in Honor of Ernest. E. Williams (A.G.J. Rhodin and K. Miyata, eds.). Museum of Comparative Zoology, Harvard University, USA.

Jenssen, T.A., and N.L. Gladson. 1984. Comparative display analysis of the *Anolis brevirostris* complex in Haiti. Journal of Herpetology 18:217–230.

Lovern, M.B., T.A. Jenssen, K.S. Orrell, and T. Tuchak. 1999. Comparisons of temporal display structure across contexts and populations in male *Anolis* carolinensis: signal stability or lability? Herpetologica 55:222–234.

Macedonia, J.M., and J.A. Stamps. 1994. Species recognition in *Anolis grahami* (Sauria, Iguanidae): Responses to video playbacks of conspecific and heterospecific displays. Ethology 98:246–264.

Macedonia, J.M., and D.L. Clark. 2001. Headbob display analysis of the Grand Cayman anole, *Anolis conspersus*. Journal of Herpetology 35:300–310.

Macedonia, J.M., and D.L. Clark. 2003. Headbob display structure in the naturalized *Anolis* lizards of Bermuda: Sex, context, and population effects. Journal of Herpetology 37:266–276.

Macedonia, J.M., D.L. Clark, L.E. Cherry, N.E. Mohamed, and B.W. Bartel. 2015. Comparison of headbob displays in gray-dewlapped and red-dewlapped populations of green anoles (*Anolis carolinensis*). Herpetologica 71:117–124.

Macedonia, J.M., D.L. Clark, M.R. Fonley, I. Centurione, J.W. Rowe, and C.A. Valle. 2019. Analysis of bobbing displays in four species of Galápagos lava lizards using conventional and novel quantitative methods. Herpetologica 74:290–300.

Macedonia, J.M., D.L. Clark, and M.R. Fonley. 2021. Analysis of bobbing displays in the *grahami* series of anoles from Jamaica and Grand Cayman. Herpetological Monographs 35:65–89.

Martins, E.P. 1993. A comparative study of the evolution of *Sceloporus* push-up displays. The American Naturalist 142:994–1018.

Martins, E.P., and J. Lamont. 1998. Estimating ancestral states of a communicative display: a comparative study of *Cyclura* rock iguanas. Animal Behaviour 55:1685–1706.

Martins, E.P., A.N. Bissell, and K.K. Morgan. 1998. Population differences in a lizard communicative display: evidence for rapid change in structure and function. Animal Behaviour 56:1113–1119.

Martins, E.P., A. Labra, M. Halloy, and J.T. Thompson. 2004. Large-scale patterns of signal evolution: an interspecific study of *Liolaemus* lizard headbob displays. Animal Behaviour 68:453–463.

Martins, E.P., A.G. Ossip-Klein, J.J. Zúñiga-Vega, C.V. García, S.M. Campos, and D.K. Hews. 2015. Evolving from static to dynamic signals: evolutionary compensation between two communicative signals. Animal Behaviour 102:223–229.

McKinney, C.O. 1971. Individual and intrapopulational variation in the push-up display of *Uta stansburiana*. Copeia 1971:159–160**.**

Nelson, C.M.V., and T.J. Ord. 2022. Identifying potential cues of species identity in complex animal signals. Animal Behaviour 186:121–136.

Nelson, C.M.V., W.B. Sherwin, and T.J. Ord. 2022. Why does the complexity of functionally equivalent signals vary across closely related species? Behavioral Ecology 33:926–936.

Ord, T.J., and E.P. Martins. 2006. Tracing the origins of signal diversity in anole lizards: phylogenetic approaches to inferring the evolution of complex behaviour. Animal Behaviour 71:1411–1429.

Ord, T.J., R.A. Peters, B. Clucas, and J.A. Stamps. 2007. Lizards speed up visual displays in noisy motion habitats. Proceedings of the Royal Society B 274:1057–1062.

Ord, T.J., J.A. Stamps, and J.B. Losos. 2013. Convergent evolution in the territorial communication of a classic adaptive radiation: Caribbean *Anolis* lizards. Animal Behaviour 85:1415–1426.

Peters, R.A., J. De Jong, and J.A. Ramos. 2022. Movement-based signalling by four species of dragon lizard (family Agamidae) from the Kimberley region of Western Australia. Australian Journal of Zoology doi:10.1071/ZO21047.

Queral, A., R. Garcia, R. Powell, J.S. Parmerlee, Jr., D.D. Smith, and A. Lathrop. 1995. Agonistic responses by a grass anole, *Anolis olssoni* from the Dominican Republic, to male conspecifics. Amphibia-Reptilia 16:313–321.

Ramos, J.A., and R.A. Peters. 2021. Territorial displays of the *Ctenophorus decresii* complex: a story of local adaptations. Frontiers in Ecology and Evolution doi: 10.3389/fevo.2021.731705.

Ruibal, R. 1967. Evolution and behavior in West Indian anoles. Pp. 116–140 in Lizard ecology: a symposium. (W. W. Milstead, ed.). University of Missouri Press, USA.

TABLE S2. Correlation matrices for unit-based variables within each study population. Correlations in bold type are significant at $P < 0.05$ in a Spearman Rank Correlation test for each population. Sixteen adult male *Microlophus bivittatus* subjects on San Cristóbal and 16 on Isla Lobos contributed one mean value for each variable from their two signature displays.

SAN CRISTÓBAL	U1 Dur	U2 Dur	U3 Dur	U4 Dur	U5 Dur	Display Dur	U1 Peak Amp	U3 Peak Amp	U5 Peak Amp
Unit 1 Duration	1								
Unit 2 Duration	0.073	1							
Unit 3 Duration	-0.053	0.243	1						
Unit 4 Duration	0.152	-0.120	-0.321	1					
Unit 5 Duration	0.198	0.407	0.276	0.129	1				
Display Duration	0.324	**0.635**	**0.773**	0.017	**0.603**	1			
Unit 1 Peak Amplitude	0.458	**0.505**	0.185	0.413	0.371	**0.614**	1		
Unit 3 Peak Amplitude	-0.184	-0.047	0.190	0.248	0.067	0.137	0.438	1	
Unit 5 Peak Amplitude	0.260	0.073	-0.042	-0.321	-0.241	-0.044	-0.484	**-0.682**	1

ISLA LOBOS	U1 Dur	U2 Dur	U3 Dur	U4 Dur	U5 Dur	Display Dur	U1 Peak Amp	U3 Peak Amp	U5 Peak Amp
Unit 1 Duration	1								
Unit 2 Duration	0.513	1							
Unit 3 Duration	0.001	-0.288	1						
Unit 4 Duration	-0.123	-0.257	0.155	1					
Unit 5 Duration	0.185	0.139	-0.316	-0.025	1				
Display Duration	**0.745**	**0.709**	0.326	0.041	0.183	1			
Unit 1 Peak Amplitude	0.173	0.483	-0.368	**-0.528**	0.001	0.099	1		
Unit 3 Peak Amplitude	-0.036	-0.121	0.241	-0.286	**-0.765**	-0.168	0.076	1	
Unit 5 Peak Amplitude	0.108	-0.120	0.157	0.081	0.403	0.139	**-0.500**	-0.418	1

TABLE S3.—Eigenvalues, percent of variance, and cumulative percent variance accounted for by four principal components with Eigenvalues > 1.0. Components extracted from 9 unit-based variables (= Display Duration, 5 unit durations, and 3 standardized peak amplitudes) used to measure bobbing display structure in 2 displays of 16 adult male *Microlophus bivittatus* subjects each on San Cristóbal and Isla Lobos.

	Rotated sums of squared loadings		
Principal component	Eigenvalues	Variance %	Cumulative %
PC1	2.050	22.781	22.781
PC2	1.805	20.054	42.834
PC3	1.683	18.695	61.529
PC4	1.540	17.110	78.639

TABLE S4.— Relationships of Varimax-rotated principal components (PCs) to six duration-based measures and three standardized peak amplitude ("peak") measures of *Microlophus bivittatus* bobbing display structure from 16 adult male subjects each on San Cristóbal and Isla Lobos. Variables with the most heavily weighted factor loadings (absolute value > 0.6) shown in bold.

	Principal Component			
Variable	1	2	3	4
Display Duration	**0.972**	0.053	0.058	-0.134
Unit 1 Duration	**0.714**	0.081	0.288	0.202
Unit 3 Peak	0.032	**-0.881**	-0.018	0.058
Unit 5 Duration	0.368	**0.678**	0.204	0.147
Unit 5 Peak	0.038	**0.636**	-0.575	0.070
Unit 1 Peak	0.327	0.005	**0.791**	0.032
Unit 2 Duration	0.527	0.236	0.574	-0.241
Unit 4 Duration	0.125	-0.086	-0.239	**0.911**
Unit 3 Duration	0.241	-0.303	-0.406	**-0.750**

TABLE S5.—Standardized canonical discriminant function coefficients, which show the relative contribution of each principal component (while controlling for the other components) to the discriminant function that classified bobbing displays to population. In this analysis, PC scores were derived from unit-based values from 2 displays of 16 adult male *Microlophus bivittatus* subjects each on San Cristóbal and Isla Lobos.

PC	Discriminant Function 1
PC1	0.601
PC2	-0.117
PC3	0.818
PC4	0.293

TABLE S6.— Eigenvalues, percent of variance, and cumulative percent variance accounted for by four principal components with Eigenvalues > 1.0. Components extracted from data means of 9 unit-based variables (= Display Duration, 5 unit durations, and 3 standardized peak amplitudes) used to measure bobbing display structure in 16 adult male subjects each from the San Cristóbal and Isla Lobos populations of *Microlophus bivittatus*.

	Rotated sums of squared loadings		
Principal component	Eigenvalues	Variance %	Cumulative %
PC1	2.246	24.953	24.953
PC2	1.903	21.143	46.096
PC3	1.652	18.354	64.450
PC4	1.530	17.003	81.452

TABLE S7.—Relationships of Varimax-rotated principal components to six duration measures and three standardized peak amplitude measures of *Microlophus bivittatus* bobbing display structure. In this analysis, data were means derived from 2 displays of 16 adult male subjects each on San Cristóbal and Isla Lobos. Variables with the most heavily weighted factor loadings (absolute value > 0.6) shown in bold.

	Principal Component			
Variable	1	2	3	4
Display Duration	**0.991**	-0.028	0.016	-0.011
Unit 1 Duration	**0.668**	0.313	0.169	0.462
Unit 2 Duration	**0.656**	0.456	0.219	-0.409
Unit 1 Peak	0.344	**0.785**	-0.038	-0.029
Unit 5 Peak	0.029	**-0.759**	0.383	0.107
Unit 3 Duration	0.352	-0.576	-0.479	-0.469
Unit 3 Peak	0.045	0.245	**-0.850**	0.080
Unit 5 Duration	0.376	0.030	**0.689**	0.172
Unit 4 Duration	0.039	-0.112	0.031	**0.939**

TABLE S8.—Standardized canonical discriminant function coefficients, which show the relative contribution of each principal component (while controlling for the other components) to the discriminant function that classified bobbing displays to population. In this analysis, data were PC scores of unit-based value means derived from 2 displays of 16 adult male subjects each on San Cristóbal and Isla Lobos.

PC	Discriminant Function 1
PC1	0.556
PC2	0.876
PC3	0.190
PC4	0.238

TABLE S9. Correlation matrices for DFT variables within each study population. Correlations in bold type are significant at $P < 0.05$ in a Spearman Rank Correlation test for each population. Sixteen adult male *Microlophus bivittatus* subjects on San Cristóbal and 16 on Isla Lobos contributed one mean value for each variable from their two signature displays.

SAN CRISTÓBAL													
Number of Variables = 13													
Observations per variable = 16													
	PrincFreq	LowPeakFreq	MidPeakFreq	HiPeakFreq	LowPartSum	MidPartSum	HiPartSum	LowPercSum	MidPercSum	HiPercSum	LowMeanAmp	MidMeanAmp	HiMeanAmp
Principal Frequency	1												
Low Peak Frequency	**0.812**	1											
Middle Peak Frequency	-0.288	-0.287	1										
High Peak Frequency	0.384	0.028	0.021	1									
Low Frequency Partial Sum	-0.328	-0.054	0.200	-0.400	1								
Middle Frequency Partial Sum	0.142	0.370	-0.398	0.031	0.156	1							
High Frequency Partial Sum	-0.160	-0.089	0.329	-0.097	0.150	-0.076	1						
Low Freq. Percentage of Sum	-0.407	-0.238	0.225	-0.384	**0.760**	-0.202	-0.255	1					
Mid. Freq. Percentage of Sum	0.221	0.250	**-0.523**	0.210	-0.405	**0.733**	-0.403	-0.338	1				
High Freq. Percentage of Sum	-0.132	-0.166	0.343	0.025	-0.175	-0.275	**0.915**	-0.370	-0.332	1			
Low Freq. Mean Amplitude	-0.193	-0.003	0.440	-0.044	0.682	0.154	-0.006	0.449	-0.332	-0.241	1		
Middle Freq. Mean Amplitude	0.298	0.332	0.064	0.265	-0.049	0.287	-0.123	-0.378	0.006	-0.229	0.474	1	
High Freq. Mean Amplitude	-0.069	-0.095	0.517	0.166	0.008	-0.349	**0.719**	-0.255	**-0.594**	**0.715**	0.304	0.294	1

ISLOTE LOBOS													
Number of Variables = 13													
Observations per variable = 16													
	PrincFreq	LowPeakFreq	MidPeakFreq	HiPeakFreq	LowPartSum	MidPartSum	HiPartSum	LowPercSum	MidPercSum	HiPercSum	LowMeanAmp	MidMeanAmp	HiMeanAmp
Principal Frequency	1												
Low Peak Frequency	**1**	1											
Middle Peak Frequency	-0.018	-0.018	1										
High Peak Frequency	0.042	0.042	-0.299	1									
Low Frequency Partial Sum	-0.569	-0.569	-0.08	-0.020	1								
Middle Frequency Partial Sum	0.137	0.137	-0.238	0.422	0.167	1							
High Frequency Partial Sum	-0.141	-0.141	0.127	-0.392	-0.003	-0.302	1						
Low Freq. Percentage of Sum	**-0.628**	**-0.628**	0.016	0.058	**0.855**	0.033	-0.329	1					
Mid. Freq. Percentage of Sum	0.213	0.213	-0.164	0.457	-0.154	**0.873**	-0.522	-0.044	1				
High Freq. Percentage of Sum	-0.106	-0.106	0.156	-0.393	-0.174	-0.388	**0.967**	-0.393	-0.487	1			
Low Freq. Mean Amplitude	-0.021	-0.021	0.067	-0.201	0.443	-0.018	0.419	0.225	-0.249	0.324	1		
Middle Freq. Mean Amplitude	**0.590**	**0.590**	-0.117	0.220	**-0.644**	0.513	-0.192	**-0.735**	**0.583**	-0.180	-0.304	1	
High Freq. Mean Amplitude	0.226	0.226	0.327	-0.335	-0.398	-0.393	**0.857**	**-0.654**	-0.490	**0.870**	0.244	0.103	1

TABLE S10.—Eigenvalues, percent of variance, and cumulative percent variance accounted for by five principal components with Eigenvalues > 1.0. Components extracted from 13 DFT variables used to measure bobbing display structure in 2 displays of 16 adult male *Microlophus bivittatus* subjects each from San Cristóbal and Isla Lobos.

	Rotated sums of squared loadings		
Principal component	Eigenvalues	Variance %	Cumulative %
PC1	3.038	23.368	23.368
PC2	2.358	18.138	41.506
PC3	2.310	17.773	59.279
PC4	2.014	15.493	74.771
PC5	1.291	9.927	84.699

TABLE S11.—Relationships of Varimax-rotated principal components to 13 DFT measures of *Microlophus bivittatus* bobbing display structure from subjects on San Cristóbal and Isla Lobos (16 males X 2 populations X 2 displays). Variables with the most heavily weighted factor loadings (absolute value > 0.6) shown in bold.

	Principal Component				
Variable	1	2	3	4	5
High Frequency Partial Sum	**0.916**	-0.054	-0.076	0.042	0.198
High Frequency Mean Amplitude	**0.914**	0.231	-0.106	0.137	-0.032
High Frequency % of Sum	**0.885**	-0.028	-0.164	-0.190	0.228
Low Frequency % of Sum	-0.525	-0.489	-0.307	0.496	0.156
Low Peak Frequency	0.004	**0.923**	0.036	-0.073	0.139
Principal Frequency	0.048	**0.913**	0.044	-0.164	-0.071
Middle Frequency Partial Sum	-0.135	-0.038	**0.951**	0.052	-0.025
Middle Frequency % of Sum	-0.305	-0.020	**0.841**	-0.325	-0.017
Middle Freq. Mean Amplitude	0.162	0.433	**0.725**	0.002	-0.262
Low Frequency Mean Amplitude	0.115	-0.019	-0.071	**0.930**	-0.004
Low Frequency Partial Sum	-0.223	-0.431	-0.063	**0.763**	0.117
High Peak Frequency	-0.107	-0.043	0.150	0.045	**-0.894**
Middle Peak Frequency	0.301	-0.023	0.017	0.349	0.516

TABLE S12.—Standardized canonical discriminant function coefficients, which show the relative contribution of each principal component (while controlling for the other components) to the discriminant function that classified bobbing displays to population. In this analysis, DFT-derived principal component scores were from 2 displays of 16 adult male subjects each on San Cristóbal and 16 on Isla Lobos.

PC	Discriminant Function 1
PC1	0.526
PC2	0.837
PC3	-0.052
PC4	-0.355
PC5	0.007

TABLE S13.— Eigenvalues, percent of variance, and cumulative percent variance accounted for by four principal components with Eigenvalues > 1.0. Components extracted from data means of 13 DFT variables used to measure bobbing display structure in 16 adult male *Microlophus bivittatus* subjects each on San Cristóbal and Isla Lobos.

	Rotated sums of squared loadings		
Principal component	Eigenvalues	Variance %	Cumulative %
PC1	3.087	23.750	23.750
PC2	3.069	23.607	47.357
PC3	2.286	17.587	64.944
PC4	1.779	13.683	78.627

TABLE S14.—Relationships of Varimax-rotated principal components (PCs) to 13 DFT measures of *Microlophus bivittatus* bobbing display structure. In this analysis, data were means derived from 2 displays of 16 adult male subjects each on San Cristóbal and Isla Lobos. Variables with the most heavily weighted factor loadings (absolute value > 0.6) shown in bold.

	Principal Component			
Variable	1	2	3	4
High Frequency % of Sum	**0.934**	-0.048	-0.194	-0.138
High Frequency Partial Sum	**0.931**	-0.082	-0.142	0.091
High Frequency Mean Amplitude	**0.867**	0.276	-0.274	0.133
Low Peak Frequency	-0.051	**0.910**	0.050	0.018
Principal Frequency	-0.064	**0.890**	0.017	-0.133
Middle Freq. Mean Amplitude	0.094	**0.701**	0.472	0.089
Low Frequency % of Sum	-0.511	**-0.693**	-0.152	0.405
Middle Frequency Partial Sum	-0.163	0.058	**0.916**	0.222
Middle Frequency % of Sum	-0.322	0.097	**0.856**	-0.178
High Peak Frequency	-0.076	0.122	0.457	-0.179
Low Frequency Mean Amplitude	0.090	0.035	-0.056	**0.927**
Low Frequency Partial Sum	-0.237	-0.600	-0.029	**0.666**
Middle Peak Frequency	0.346	0.050	-0.348	0.359

TABLE S15.—Standardized canonical discriminant function coefficients, which show the relative contribution of each principal component (while controlling for the other components) to the discriminant function that classified bobbing displays to population. In this analysis, data were PC scores of DFT value means derived from 2 displays of 16 adult male subjects each on San Cristóbal and Isla Lobos.

PC	Discriminant Function 1
PC1	0.456
PC2	0.888
PC3	-0.229
PC4	-0.290

Captions for Supplemental Image and Videos

Supplemental materials for this paper can be viewed and downloaded at https://www.macedonialab.com/publications.html.

Image S1.—Video screen capture of an Isla Lobos *Microlophus bivittatus* adult male next to a male conspecific-mimicking (San Cristóbal) robot for scale. The robot was fashioned to be the average size of males at Puerto Baquerizo Moreno (SVL = 74 mm). The box on which the live and robotic male are perched houses the mechanical and electronic components that allow the robot to perform signature bobbing displays. See Clark et al. (2023: cited in the paper) for details.

Video S1.—Video of an Isla Lobos *Microlophus bivittatus* adult male next to a male conspecific-mimicking robot. The real male performs a single signature display, which is followed by the robot performing one signature display. The robot is the same size as an average adult male (SVL = 74 mm) from San Cristóbal.

Video S2.—Video of an Isla Lobos *Microlophus bivittatus* adult male performing three signature displays with a male conspecific-mimicking robot in the foreground.

Video S3.—Video of a San Cristóbal adult male performing three signature displays.

Video S4.—Video of a second San Cristóbal adult male performing three signature displays.